Research paper

The Holocene
1–14

DOI: 10.1177/0959683616675938
hol.sagepub.com
SAGE

The Bengal fan: External controls on the Holocene Active Channel turbidite activity

Léa Fournier,[1] Kelly Fauquembergue,[1] Sébastien Zaragosi,[1] Coralie Zorzi,[2] Bruno Malaizé,[1] Franck Bassinot,[3] Ronan Joussain,[4,5] Christophe Colin,[5] Eva Moreno[6] and François Leparmentier[7]

Abstract

The eastern levee of the Active Channel in the Bengal fan has been investigated in order to better understand the history of turbidite activity in this channel during the Holocene in the context of Ganges-Brahmaputra 'source-to-sink' system. A robust ^{14}C-based chronostratigraphy provides high temporal resolution for reconstructing sediment accumulation history on the eastern levee of the Active Channel. Integration of this study with previous work in the area suggests that the Bengal fan has remained continually connected with the Ganges-Brahmaputra fluvial system through the Holocene, feeding through the main canyon, the Swatch of No Ground (SoNG). An intense turbidite activity occurred during a transgressive wet period from 14.5 to 9.2 ka cal. BP, followed by an abrupt shift in sedimentation at 9.2 ka cal. BP, probably due to the high sea level leading to a partial disconnection between massive river discharges and the deep turbidite system. During the last 9.2 ka cal. BP, turbidite activity is still present but irregular, likely modulated by a combination of various forcings such as monsoon variability and river migration. In total, three phases are distinguishable during this period: 9.2–5.5, 5.5–4, and 4 ka cal. BP to modern, according to the turbidite record. Unexpectedly, the Indo-Asian monsoon does not appear to be the only predominant forcing on the establishment of the Bengal fan during the Holocene because of the combination of different forcings directly affecting transfers between the Ganges-Brahmaputra and the Bengal fan as well as river migrations, delta construction, and potentially anthropogenic impact.

Keywords

Bengal fan, Holocene, Indo-Asian monsoon, river migration, sea level, turbidite activity

Received 18 March 2016; revised manuscript accepted 27 September 2016

Introduction

Ganges-Brahmaputra rivers and their trans-Himalaya tributaries drain a vast area of about 1,830,000 km^2, from Himalaya and Central Tibet to the Meghna estuary in Bangladesh (Figure 1). Their sedimentary discharges are estimated at around 1×10^9 t/an (Milliman and Syvitski, 1992) mainly because of intense rainfall during the Indian summer monsoon. The modern sedimentary budget of the Ganges-Brahmaputra river delta is partitioned between (1) the floodplain (30%), (2) the subaqueous delta (40%), (3) the coastal delta plain (10%), and (4) the main submarine canyon (the Swatch of No Ground (SoNG)) and the Bengal fan (20%; Goodbred and Kuehl, 1999, and publications therein; Rogers et al., 2013).

The SoNG is the main connection between the sediment source and the Ganges-Brahmaputra turbidite system, known as the Bengal fan (Curray et al., 2003). It is a shelf-incising aggrading canyon. The head of the canyon is located 150 km from the modern Ganges and Brahmaputra mouths and only 30 km from the coastal delta plain (Figure 1). The upper canyon floor reveals a massive storage of sediments with a sedimentation rate between 8 and 50 cm/yr (Kudrass et al., 1998; Kuehl et al., 1989). A recent study (Rogers et al., 2015) presents three main mechanisms which can explain sediment transport between the 'widely separated' Ganges-Brahmaputra mouths and the canyon head: (a) rapid progradation of the subaqueous delta, (b) mass failures, and (c) bypass gully systems from the inner shelf to the canyon conveying sediment gravity flows.

Transfer of sediment from the SoNG to the Ganges-Brahmaputra turbidite system has remained active throughout the Holocene and modern time period (Weber et al., 1997). The slowdown of the sea-level rise around 7 ka cal. BP (Goodbred and Kuehl, 2000a) associated with huge sediment discharges has supported the southward progradation of the subaqueous delta on the shelf, with a modern rate of 15–20 m/yr (Hubscher et al., 1997; Kuehl et al., 1997).

At the present time, there is only one Active Channel (named AV for 'Active valley' by Curray et al., 2003) connected to the

[1]UMR CNRS 5805 EPOC, Université de Bordeaux, France
[2]Department of Earth and Atmospheric Sciences, UQAM, Canada
[3]Laboratoire des Sciences du Climat et de l'Environnement (LSCE/IPSL), UMR 8212 CNRS-CEA-UVSQ, France
[4]State Key Laboratory of Marine Geology, Tongji University, China
[5]Université Paris-Saclay, CNRS, Université Paris Sud, GEOPS, France
[6]Institut des Sciences de la Terre de Paris (iSTeP), Muséum national d'histoire naturelle (MNHN), Sorbonne Universités, France
[7]Département Bassins et Thématiques Frontières, Direction Exploration/Division Projets Nouveaux, TOTAL SA, France

Corresponding author:
Léa Fournier, UMR CNRS 5805 EPOC, Université de Bordeaux, Bâtiment B18, 33615 Pessac Cedex, France.
Email: l.fournier@epoc.u-bordeaux1.fr

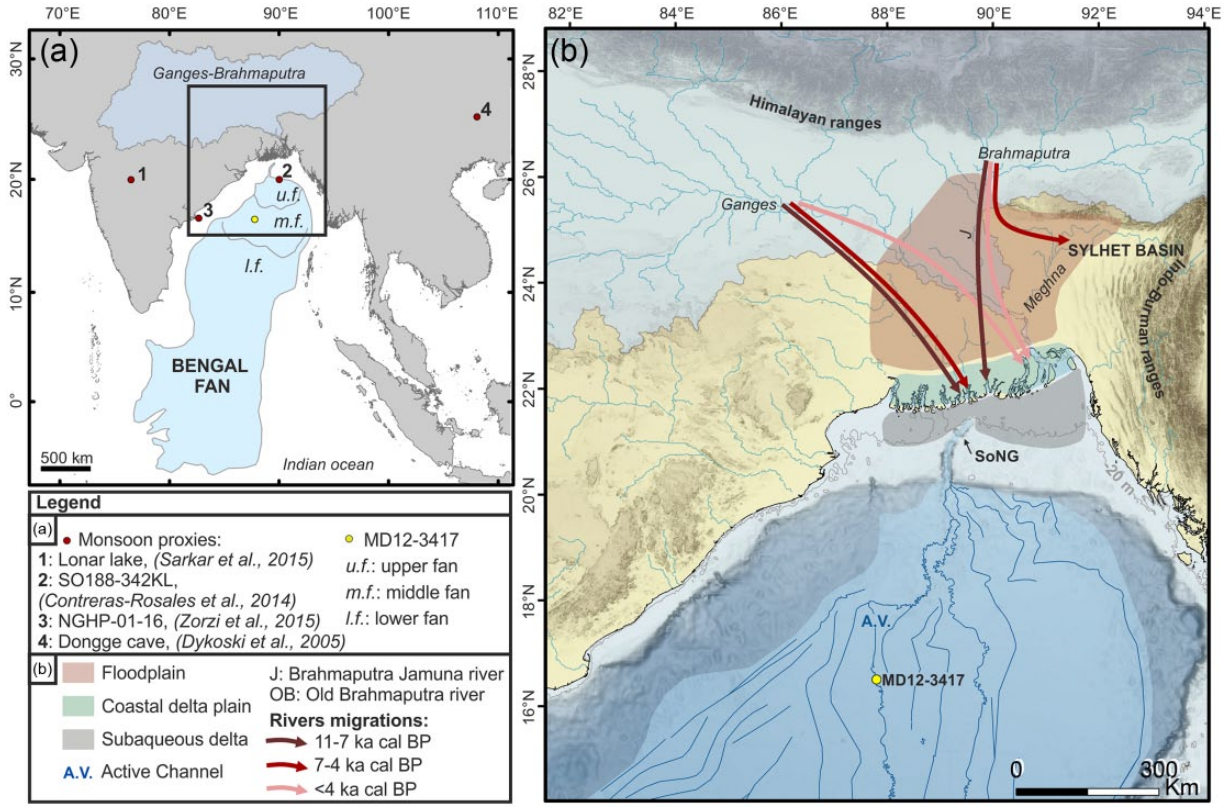

Figure 1. (a) Location map and physiography of the Ganges-Brahmaputra sedimentary system, from source to sink. Location of the monsoon proxies used in this study. (b) Zoom in the transition area between the Ganges-Brahmaputra fluvial system, the subaqueous delta, the SoNG, and the northern Bengal fan. Using Goodbred and Kuehl (2000b), location of the floodplain, the coastal plain and the subaqueous delta have been estimated. The gray line represents the position of the sea level at 9.2 ka cal. BP (e.g. −20 m), according to the global sea-level curve (Lambeck et al., 2014). SoNG: the Swatch of No Ground canyon. Channel location in the Bengal fan is obtained from several studies combined (Curray et al., 2003; Kolla et al., 2012; Thomas et al., 2012; NoAA database: http://www.ncdc.noaa.gov/; 2012 MONOPOL cruise bathymetry; personal TOTAL seismic lines interpretation). Arrows represent the global Ganges-Brahmaputra river positions during the Holocene, according to Goodbred et al. (2014) and Pickering et al. (2014).

SoNG (Figure 1). This Active Channel has been studied by Weber et al. (1997) and Hubscher et al. (1997) with piston cores and high-resolution 3.5-kHz seismic profiles. Its initiation has been dated around 14.5 ka cal. BP (12.8 ka ^{14}C yr BP in Weber et al., 1997).

Our study focuses on sediment cores located on the eastern levee of the Active Channel. We present a detailed record of turbiditic activity across the Holocene with a special focus on changes in turbiditic frequencies. Similar studies have been already performed on other turbidite systems in the world, such as the Indus turbidite system (Bourget et al., 2013), the Armorican turbidite system in the Northern Atlantic (Toucanne et al., 2012), or the Var turbidite system in the Mediterranean Sea (Bonneau et al., 2014).

This study provides a new insight on the main forcing parameters, which affect the construction of the Active Channel and will integrate the significance of the eustatic/monsoonal variations combined on the construction of the Ganges-Brahmaputra turbidite system during the Holocene.

Background

A large source-to-sink system such as the Ganges-Brahmaputra turbidite system comprises all areas that contribute to erosion, transportation, and deposition of sediments within an erosional–depositional system, from catchment to the deep sea fan (Sømme et al., 2009). To understand the development of a source-to-sink system, a global perspective is required, including a combination of autogenic and allogenic forcings and a good understanding of the sediment distribution in response to those forcings (Sømme et al., 2009).

These forcings as well as tectonic activity, monsoonal variations, and sea-level fluctuations impact the entire Ganges-Brahmaputra turbidite system and have consequences on the river migration, the construction of the delta, and on the deep sea fan sedimentation (Sømme et al., 2009).

Ganges-Brahmaputra fluvial system and its delta are tectonically influenced by the main Himalayan and Indo-Burman ranges (Alam, 1989; Morgan and McIntire, 1959), and numerous earthquakes and paleoearthquakes have been identified during the Holocene (Anand and Jain, 1987; Kumar et al., 2006; Mugnier et al., 2011; Singh et al., 1997; Wang et al., 2014).

Several landslides have been studied in Himalaya and on the Tibetan plateau and have been linked to paleoseismic events during the Holocene (Dortch et al., 2011; Mugnier et al., 2011; Wang et al., 2014). Tectonic events (e.g. 1950 earthquake in Assam, India; Poddar, 1952) had major effects on the Brahmaputra tributaries course, the fast progradation of the river-mouth shoreline, and a rapid widening of the river braidbelt (Goodbred et al., 2003; Pickering et al., 2014). Tectonic activity also affected the delta system during the late Quaternary, particularly in the eastern part with tectonic uplift and subsidence, which constrained and shaped its construction and resulted in sediment trapping (Goodbred et al., 2003). Regional subsidence in the Bengal basin directly affected the rate, magnitude, and characteristics of sediments delivered by rivers (Goodbred et al., 2003) and the evolution of the delta plain, during the late-Holocene (Allison et al., 2003). The floodplain and the coastal delta plain are dominated by plate-driven tectonic processes that cause subsidence reaching 4 mm/yr (Goodbred and Kuehl, 2000b). Recently, Reitz et al. (2015) presented the idea of possible influence of regional subsidence on

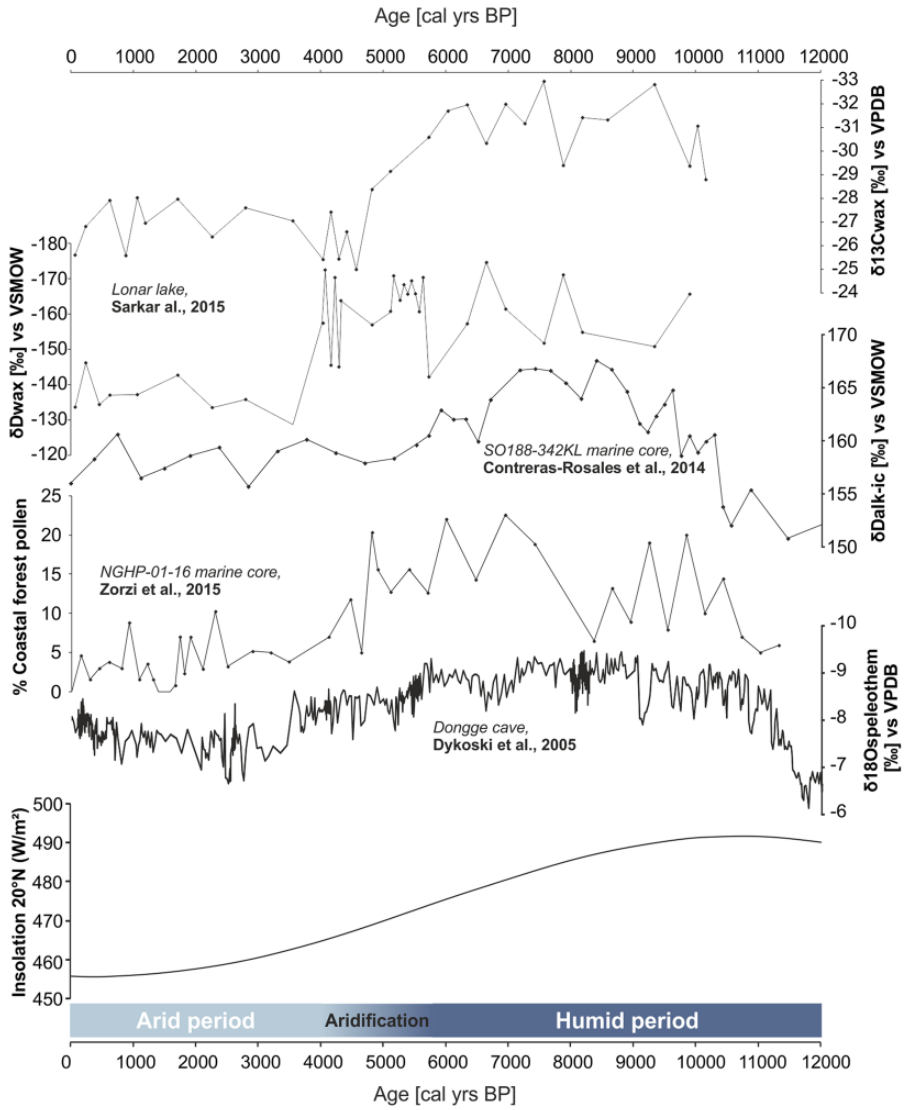

Figure 2. Holocene Indo-Asian monsoon variability: comparison of the records: Lonar lake $\delta^{13}C$ and δD records (Sarkar et al., 2015), δD record from sediment core SO188-342KL (Contreras-Rosales et al., 2014), percentage of coastal forest pollen record from sediment core NGHP-01-16 (Zorzi et al., 2015), Dongge cave speleothem $\delta 18O$ record (Dykoski et al., 2005), and insolation curve at 20°N.

river avulsions (avulsion timescale around 2000 years) and Ganges-Brahmaputra delta construction. In the subaqueous delta, transparent units have been presented as evidence of liquefaction flows, generated by earthquakes (Palamenghi et al., 2011). Storms and earthquakes contribute to sedimentation in the SoNG and Bengal fan (Kottke et al., 2003), but it is difficult to establish a clear link between an event and a deposit especially in the deep system (Bourget et al., 2010; Goldfinger et al., 2007). If earthquakes are important triggers of delta sedimentation, they could also be important triggers for the deep sedimentation through the SoNG.

In addition to tectonic activity, climatic variability and the distribution of monsoon precipitation, as well as eustatic variations, strongly influenced Ganges-Brahmaputra river migration, Ganges-Brahmaputra delta construction, and deep sedimentation in the Bengal fan during the Holocene (Goodbred et al., 2003).

The Indo-Asian monsoon variability has been well documented with the development of high-resolution paleoclimatic records (marine as well as continental records) that provide a long-term perspective of the evolution of monsoon precipitation, in particular during the Holocene, the time period studied in this work (Berkelhammer et al., 2012; Cai et al., 2012; Contreras-Rosales et al., 2014; Dykoski et al., 2005; Sarkar et al., 2015; Zorzi et al., 2015; Figure 2). Paleoclimate studies based on multiproxy approaches revealed a significant change in monsoon during the Holocene, with a transition between a wet early-Holocene and an arid late-Holocene (Berkelhammer et al., 2012; Cai et al., 2012; Contreras-Rosales et al., 2014; Dykoski et al., 2005; Sarkar et al., 2015; Zorzi et al., 2015). The climate evolution across the Holocene is thus characterized by (a) a very humid period between 11 and 6 ka cal. BP, (b) a weakening of the monsoon between 6 and 4 ka cal. BP, and (c) a relatively less humid period during the last 4 ka cal. BP (Sarkar et al., 2015; Zorzi et al., 2015). Several studies in the Bay of Bengal suggest that millennial scale variations in the monsoon have possible teleconnection climate variations in Greenland climate (Kudrass et al., 2001; Weber et al., 1997).

Holocene monsoon variations are combined with global sea-level fluctuations recorded by shoreline indicators which highlight a main phase of deglaciation between 16.5 and 8.2 ka cal. BP at an average of 12 m/ka BP and a progressive decrease in the rate of rise from 8.2 to 2.5 ka cal. BP (Lambeck et al., 2014). The Ganges-Brahmaputra major sediment load was able to keep pace with rapid sea-level rise during this period (Goodbred and Kuehl, 2000b). In the Bay of Bengal, this rapid sea-level rise is recorded in Bangladesh and India, and it is reconstructed using bore holes (Umitsu, 1993), coastal ironstone; channel fill facies (Banerjee, 1993); pollen analysis (Hait and Behling, 2008; Islam and Tooley,

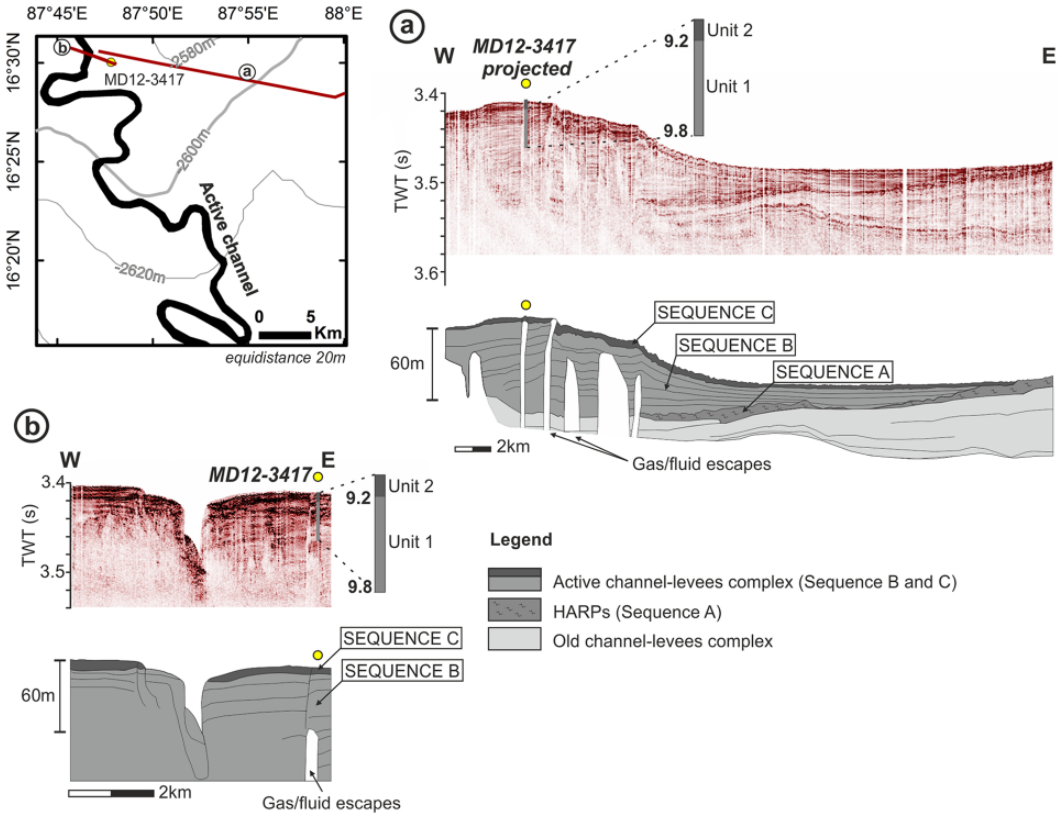

Figure 3. Schematic map with location of the core MD12-3417 and seismic profiles: the Active Channel has been drawn according to the multibeam bathymetry obtained during the MONOPOL cruise (2012). Sub-bottom seismic lines with interpretations: (a) through the eastern levee; (b) across the thalweg.

1999); and pollen, diatom, and facies analysis (Rashid et al., 2013). Islam and Tooley (1999) highlighted a first transgression phase between 9.2 and 6.8 ka BP which is also recorded more recently with a flooding of mangroves at this time in Bangladesh (Hait and Behling, 2008).

Initiation of the Ganges-Brahmaputra delta began around 11 ka cal. BP, while sea level was still rising rapidly (Goodbred and Kuehl, 2000b; Grant et al., 2012; Lambeck et al., 2010, 2014). The rapid sea-level rise was offset by massive sediment discharges of the Ganges-Brahmaputra river due to an enhanced Indo-Asian monsoon during the early-Holocene (Pate et al., 2009). From 11 to 7 ka cal. BP, the Ganges-Brahmaputra delta had been aggrading and the system became prograding after 7 ka cal. BP (Goodbred and Kuehl, 2000a).

Major fluvial channel movements have occurred during the Holocene (Goodbred et al., 2014). The Ganges river shifted eastward through the mid-Holocene to late-Holocene, and the Brahmaputra river showed a three-step evolution during the Holocene with a shift between Brahmaputra–Jamuna valley and the old Brahmaputra valley system (Goodbred et al., 2014; Pickering et al., 2014). Its migration resulted from the combination of the Indo-Asian monsoon variations and the active Himalayan uplift (Goodbred et al., 2014; Pickering et al., 2014; Figure 1).

The Ganges-Brahmaputra turbidite system extends from 20°10′N to 5°S on an area around 3×10^6 km^2 (Curray et al., 2003; Figure 1). Its dimensions make it the largest turbidite system in the world with a maximum thickness of 16.5 km. It was probably initiated during the early Eocene (Emmel and Curray, 1983).

Several channel-levee systems were built in the Bengal fan during the Quaternary, but only one seem to be connected to the SoNG at the present time (Curray et al., 2003). According to Weber et al. (1997), Hubscher et al. (1997), and Curray et al. (2003), the Active Channel has been in development since 14.5 ka cal. BP on an erosive surface. External levees were built between 14.5 and 10.4 ka cal. BP at high sedimentation rates (1–3 m/ka; Weber et al., 1997). The large channel has been infilled by inner levees constructed before 6.4 ka cal. BP, attesting to the turbidite activity during the last sea-level rise. Moreover, turbidite activity was still recorded during the last 6.4 ka cal. BP with 7 m of sediment deposited on the top of the inner levees despite the apparent disconnection between the SoNG and river mouths (Weber et al., 1997).

The authors concluded that the Ganges-Brahmaputra turbidite system is unique because of its continuous activity during the Holocene, despite the distance between the head of the canyon and the Ganges-Brahmaputra mouths (Hubscher et al., 1997; Weber et al., 1997). In order to understand the significance of sea-level and monsoon variations, sometimes in phase and sometimes out of phase, we investigate the study of marine core, located on the Active Channel-levee system.

Material and methods

Dataset

Sub-bottom seismic lines and sediment cores were obtained during the MONOPOL cruise of the R/V *Marion Dufresne in 2012*. These data have been collected in the middle Bengal fan between 2580 and 2620 m water depth, at a distance of ~780 km from the Ganges-Brahmaputra outlet (Figure 1). Sub-bottom seismic lines were obtained using a 3.5-kHz sub-bottom hull mounted profiler (Figure 3).

Sediment cores

One Calypso-long piston core (MD12-3417; 16°30.03′N; 87°47.82′E; water depth: 2564 m, 39.77 m long) and one Calypso square (CASQ) gravity core located on the same site (MD12-3418CQ; 16°30.27′N; 87°47.92′E; water depth: 2557 m, 8.52 m

Table 1. Radiocarbon ages of cores used in this study. Date in italics is date not incorporated in age model.

Core	Sample depth (cm)	Corrected sample depth (cm)	^{14}C age (yr BP)	Error (yr BP)	Calibrated age BP (years)	Error (yr cal. BP)
MD12-3418 CQ	0	0	Modern		−55	1.5
MD12-3418 CQ	205	205	1600	30	1159.5	86.5
MD12-3418 CQ	423	423	2990	30	2771.5	62.5
MD12-3418 CQ	628	628	3945	30	3942.5	104.5
MD12-3418 CQ	830	830	6705	35	7233	77
MD12-3417	*707*	*399.2*	*3290*	*30*	*3119.5*	*105.5*
MD12-3417	779	460.6	3390	30	3255.5	90.5
MD12-3417	992	662	5335	30	5703.5	109.5
MD12-3417	1074	733	5955	30	6362	75
MD12-3417	1385	1089.3	8580	40	9233	138
MD12-3417	2015	1835.3	8825	35	9479.5	55.5
MD12-3417	2186	2037.2	8870	35	9524	76
MD12-3417	2726	2677.2	9030	35	9713.5	147.5
MD12-3417	3777	3921.2	9105	35	9845	170

long) have been collected during MONOPOL cruise. These cores are located on the eastern levee of the Active Channel (Figure 1).

The Calypso piston corer induces oversampling on the upper part of the core (Skinner and McCave, 2003). To correct for oversampling, a composite record combining the Calypso and CASQ records has been done. This composite record was achieved by correlating x-ray fluorescence (XRF) data of cores MD12-3417 and MD12-3418CQ. Afterward, the depth scale of core MD12-3417 was converted to the depth scale of core MD12-3418CQ.

AMS-^{14}C dating

In total, 14 radiocarbon ages were obtained on mixed planktonic foraminifera picked in hemipelagic facies on 1-cm sediment slices except from the top of the core (5-cm sediment slice) for MD12-3418CQ and MD12-3417. Analyses have been realized at the 'Laboratoire de Mesure du Carbone 14' in Saclay (France) through the Artemis Accelerator Mass Spectrometry facility (Table 1). Radiocarbon dates are calibrated using MARINE13 curve (Reimer et al., 2013) and using a standard reservoir age of 400 years, which is close to usual corrections known for the Bay of Bengal (Dutta et al., 2001; Southon et al., 2002). The age model was constructed using the R software package Clam (version 2.2; Blaauw, 2010), with a linear interpolation method at 1-cm resolution (Figure 4).

In order to compare with previous studies, we calibrated all radiocarbon dates used in previous publication (Weber et al., 1997) using MARINE13 curve and the standard reservoir age of 400 years (Reimer et al., 2013).

Sedimentological analyses

Sedimentological analyses included visual description, high temporal resolution of XRF elementary, and high-resolution grain size study.

Lab color space measurements were performed at 2-cm resolution using a Minolta CM-2002 spectrophotometer. The color component used in this study is a*. a* negative values indicate sediment heading toward green, while positive values indicate sediment heading toward red.

Magnetic susceptibility was obtained using a Bartington™ MS2E1 pointer sensor with 10-mm resolution and a sampling interval of 10 mm.

XRF geochemical data were obtained directly on the surfaces of split cores at 1-cm resolution, using an Avaatech XRF core scanner (UMR EPOC). The measurements were performed at 10 kV and 400 µA to obtain intensities for titanium (Ti) and calcium

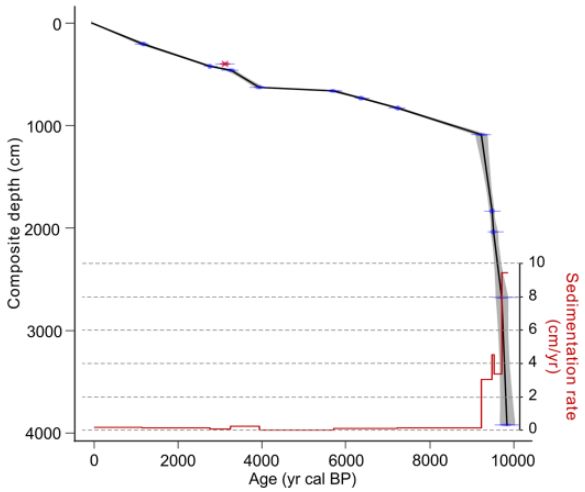

Figure 4. Age model (black line) and its error margin (gray area) of the composite core and sedimentation rate associated. Removed date is in red and crossed out.

(Ca) and at 30 kV and 1500 µA for zirconium (Zr) and rubidium (Rb). In this paper, we will discuss relative variations using element ratio to minimize the influence of sediment porosity and water content. Zr/Rb is used to indicate grain size variations (Dypvik and Harris, 2001) and particularly to identify the base of turbidite sequences (Croudace et al., 2006). Ti/Ca is commonly used to compare the siliciclastic fraction (Ti) and the biogenic fraction (Ca) and has been used to show the relative contribution of terrigenous input in deep ocean sediments (St-Onge et al., 2007). In our data, Ti/Ca shows a clear contrast between turbidites and hemipelagic material, with noticeably lower values of the Ti/Ca ratio within the turbidite sequences (Figure 5). Titanium in sediment is mainly associated with clay minerals (Wedepohl and Correns, 1969). Calcium is slightly more concentrated in turbidite sequences because of the presence of detrital calcite, and the Ti/Ca XRF ratio indicates fine-grained turbidite sequences in this study.

A high-resolution grain size study was performed using a Malvern Supersizer 'S' (UMR EPOC). Sampling has been achieved taking into account sedimentological structures: homogeneous deposits were sampled every 50 mm, whereas heterogeneous deposits were sampled at a higher resolution, ranging between 5 and 20 mm. Using this method, 1904 samples have been analyzed. The total grain size distribution versus depth is represented in Figure 5. The color scale indicates relative abundance of

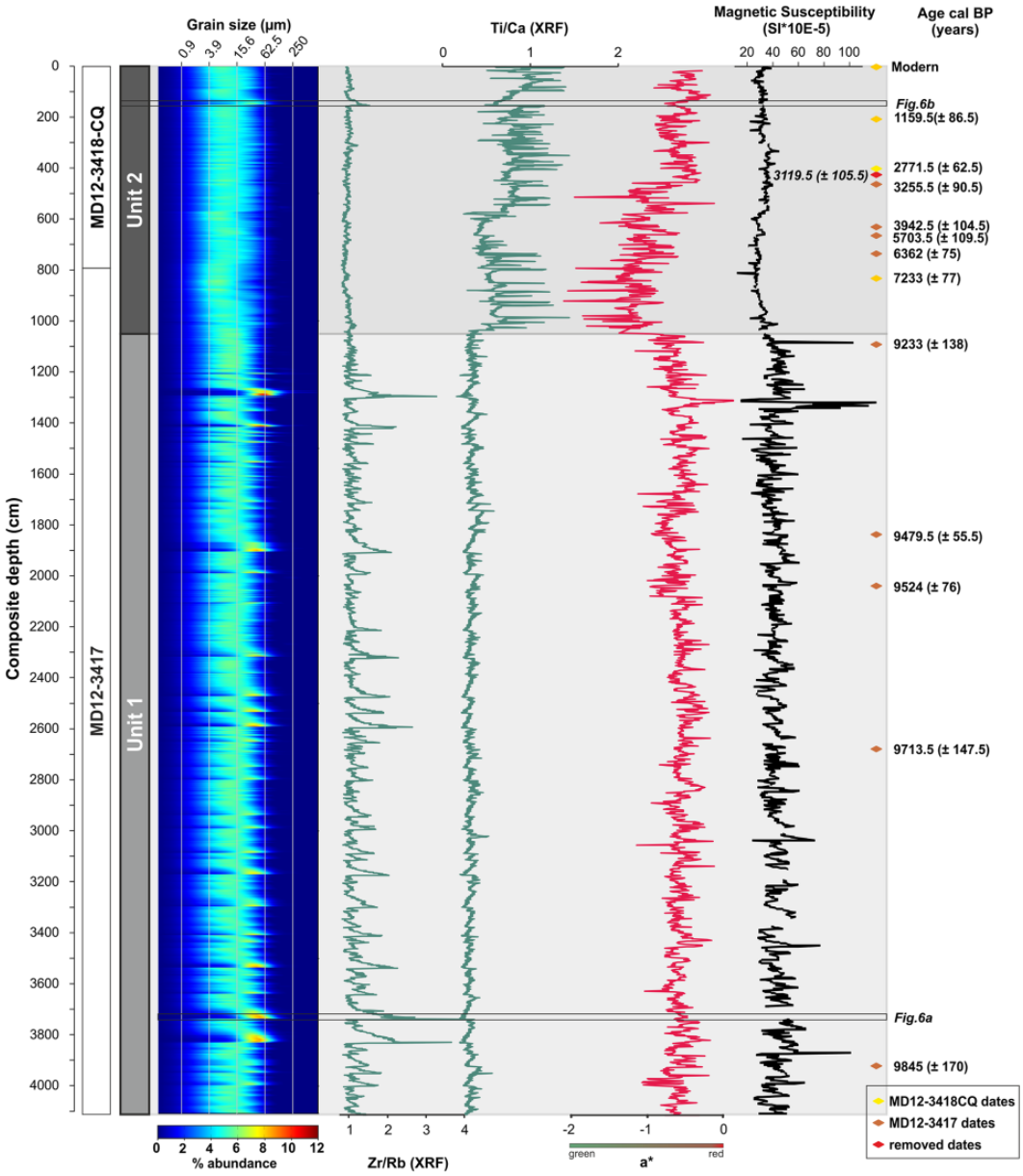

Figure 5. Grain size distribution, Zr/Rb and Ti/Ca ratios, a* (color variations, from green to red), magnetic susceptibility, and calibrated ages. Depths are composite depths (cm). Recognized units 1 and 2 are indicated to the left.

several grain size fractions (in %, from blue to red; Figure 5). Total grain size distribution shows coarser sedimentary deposits and allows identifying turbidite sequences.

Turbidite is commonly described as fining-up deposit characterized by an erosive base and typical sedimentary sequences in the deposit (Bouma et al., 1962). Recognition of turbidite is based on visual description, x-ray imagery, Ti/Ca and Zr/Rb (XRF ratio), and high-resolution grain size study.

Petrographic observations and insights into microscopic-scale sedimentary features were derived from visual observations with a Leica™ DM6000 B digital microscope on thin sections of remarkable sequences (Figure 6). Thin sections were obtained after induration of sedimentary material with a resin according to the methodology described by Zaragosi et al. (2006).

Pollen analysis was performed following the protocol established at the UMR EPOC, University of Bordeaux (http://ephe-paleoclimat.com/ephe/Pollen%20sample%20preparation.htm). Pollen identification was based on the reference collection at the French Institute of Pondicherry. We analyzed the pollen assemblages in four turbidites. Quantification was realized at 400× and 1000× (oil immersion) magnifications using Leica DFC295 microscope at the UMR EPOC. It is a qualitative approach, used to distinguish the pollen grains preservation and nature in turbidite deposits. Given the strong changes in pollen grains preservation in the sediment, the shape of the grain is used to trace the importance of transport processes affecting the sediments from the source to the Bengal fan.

Results

Chronological framework

In total, five radiometric dates were obtained on the core MD12-3418CQ and nine on the core MD12-3417 (Table 1; Figure 5). The composite core made it possible to set up an accurate age model. Ages range from modern to 9845 ± 170 yr cal. BP. One date was removed at 399 cm because of an age reversal (Table 1 and Figure 4, italic date) which can be explained by reworked foraminifera causing an aging of the sample.

An abrupt change in the sedimentation rate takes place at 1089 cm (which corresponds to an age of 9.2 ka cal. BP; Figure 4). Based on these observations, we can divide the composite core

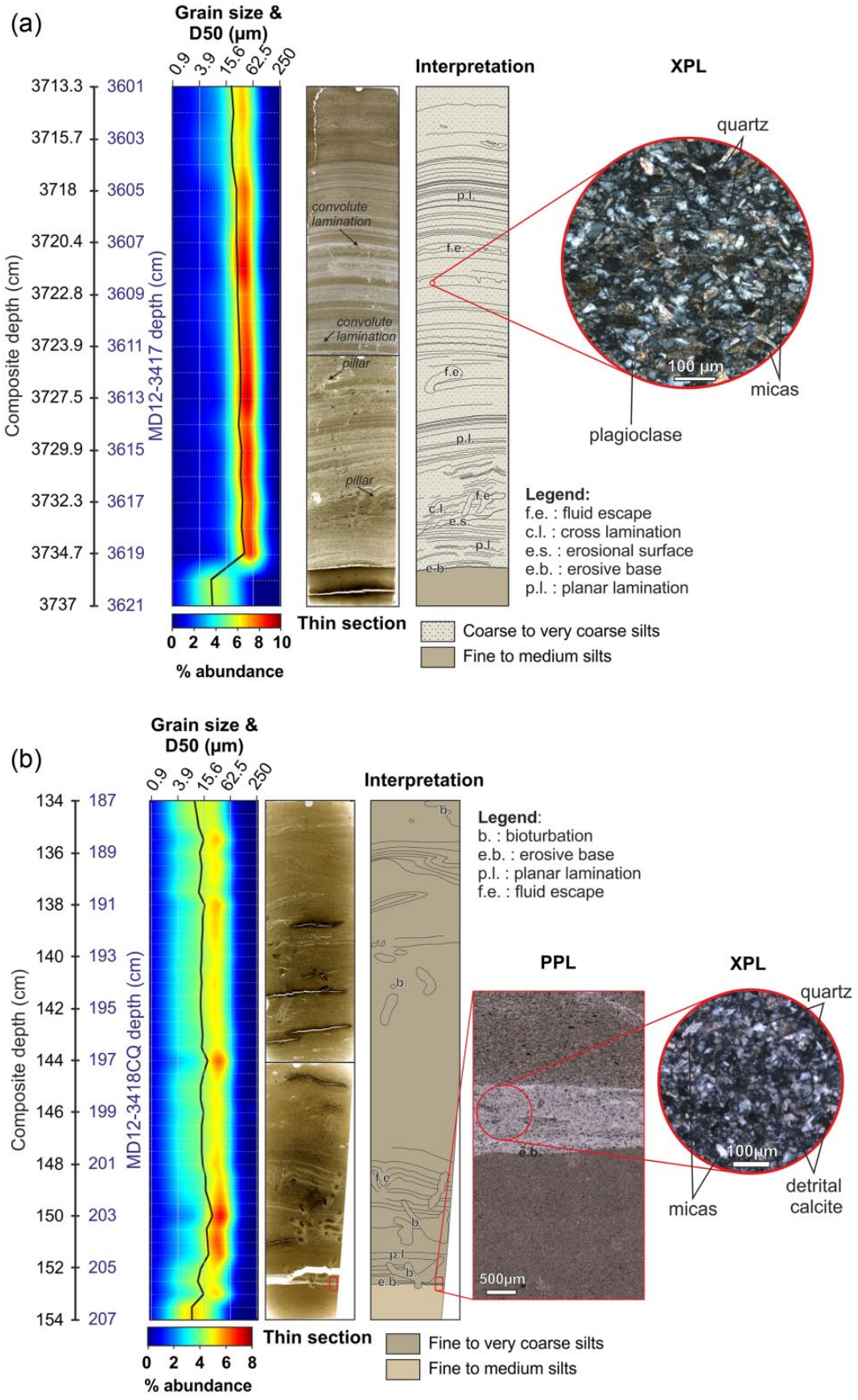

Figure 6. Example of turbidite deposits in units (a) 1 and (b) 2. Grain size distribution and D50, thin section and its interpretation, and zoom in XPL (crossed polarized light).

into two sedimentary units: unit 1 between 4113 and 1089 cm (9862–9226 yr cal. BP) with a mean sedimentation rate of 5 cm/yr and unit 2 between 1089 cm and the top (9226 yr cal. BP to modern) with a mean sedimentation rate of 0.12 cm/yr.

Sedimentological description

The grain size distribution, Zr/Rb and Ti/Ca (XRF ratios), a* color, and magnetic susceptibility records highlight the two sedimentological units described above very well (Figure 5). The total

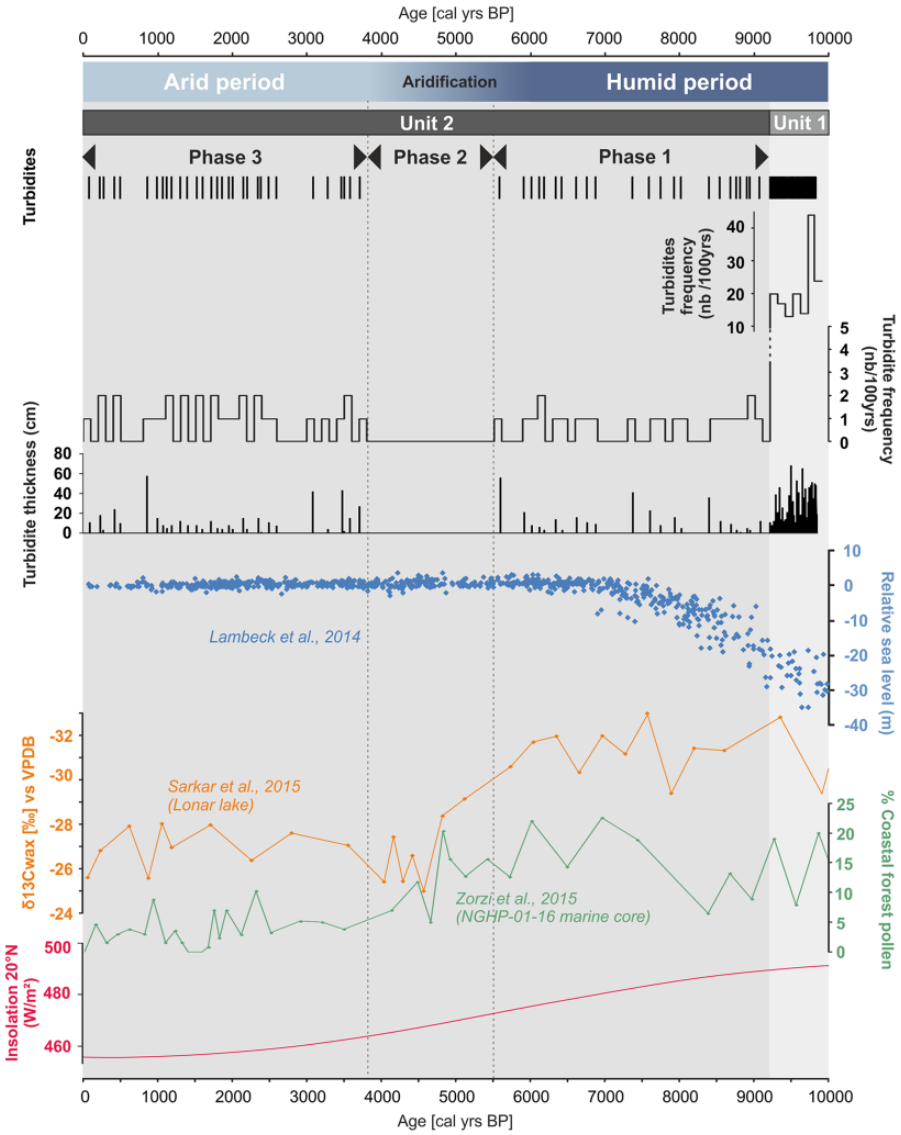

Figure 7. Correlation between Indo-Asian monsoon, global sea level, turbidite frequency, and turbidite thickness during the last 10 ka cal. BP.

grain size distribution is unimodal all along the composite core, and the sediment is relatively well sorted. Zr/Rb and Ti/Ca ratios vary by 6 and 8 in order of magnitude, respectively (Figure 5). a* color shows variations in color between −2.1 and 0.13, corresponding to a variation color of sediment between dark gray to olive (Figure 5). The magnetic susceptibility varies by approximately 10 orders of magnitude (Figure 5).

Unit 1 (from 4113 to 1089 cm). According to the age model, this unit covers an age interval between 9862 yr cal. BP (±200 years) and 9226 yr cal. BP (±140 years).

The total grain size distribution does not show any fining-up trend in unit 1 but highlights the presence of numerous coarse excursions of fine sand and fine silt above the background sedimentation (Figure 5). All excursions are well marked in the Zr/Rb XRF ratio, with an abrupt increase in the ratio at the base and a slowly upward decrease in the deposit, corresponding to a decrease in grain size. The Ti/Ca XRF ratio shows little variations in this unit.

These deposits were considered as turbidite sequences based on the recognition process described previously. We counted a total of 152 similar turbidites in unit 1 and estimated their individual thickness (Figure 7).

One excursion was studied in detail (between 3601 and 3621 cm; core depth in Figure 6a, location in Figure 5). The base of this studied turbidite is clearly erosive with a sharp transition between clayey hemipelagic sediment and medium silts in the turbidite. The turbidite base is characterized by coarse sediment ranging between very coarse silts and medium sand. The thin section shows a succession of planar and cross laminations, typical of turbidite deposits. Laminations are cut by fluid escapes as convolute laminations or pillars, which are common in coarse turbidite deposits (Lowe, 1975).

A focus in the thin section makes it possible to identify the main components which are quartz and micas, associated with some plagioclase (Figure 6a).

Pollen analysis carried out in three of these turbidites (including the turbidite presented in Figure 6a) showed essentially very poorly preserved pollen grains which could not be associated with a specific ecological group. The poor state of preservation clearly indicates that pollen grains have been extensively reworked and reflect an important transport of the detrital sediments before the deposit.

On the basis of our age model, the turbidite frequency was estimated from the composite core over 100-year interval steps (Figure 7). In unit 1 (from 9.8 to 9.2 ka cal. BP), the left levee of the Active Channel is characterized by a very high turbidite frequency, ranging from 13 to 44 turbidites per 100 years. Turbidite thickness exhibited a significant variability, ranging from 1 to 68 cm, with almost 100 turbidites thinner than 10 cm and 50 turbidites thicker than 10 cm (Figure 7).

Unit 2 (from 1089 cm to the top). Unit 2 was dated between 9226 yr cal. BP (±140 years) and the modern. The total grain size distribution varies between fine silt and very coarse silt in unit 2 (Figure 5). The grain size and Zr/Rb XRF ratio do not show the same excursions as in unit 1, and it is mainly because of the finer grain size in this unit. However, strong changes are visible within the Ti/Ca XRF ratio and are coeval with changes in the total grain size distribution.

Focusing on one of these fine excursions (between 187 and 207 cm; core depth in Figure 6b), an erosive base marked by a transition from fine/medium silts to very coarse silts is observed. This erosive base is visible when looking at the magnified thin section, which also makes it possible to identify detrital particles as quartz, micas, and detrital calcite. In this excursion, planar laminations are also visible, with liquefactions and fluid escapements in the thin section which strengthened the idea of a massive deposit of fine terrigenous particles, considered as fine-grained turbidites. Bioturbations are also visible in the deposit (Figure 6b).

The detailed study of Ti/Ca XRF ratio and the total grain size distribution enabled the identification of 54 such fine-grained turbidites in unit 2.

Pollen analysis carried out in the turbidite sequence (Figure 6b) revealed the presence of major humid species from the coastal area, attesting coastal forest, marshland, and mangrove swamps. Pollen grains are well preserved and fresh, which attests limited reworking during the transport of the sediment. The anomalous high concentration of major humid species as Borassus suggests a sediment transport from the alluvial and the coastal plain to the Bengal fan.

At 9.2 ka cal. BP, there is a drastic change in turbidite frequency, which drops to only 0–2 turbidites per 100 years (Figure 7). As in unit 1, the thickness of individual turbidites shows variability, ranging from 1 to 57.5 cm, with an equal distribution between fine and thick turbidites (29 turbidites thinner than 10 cm and 25 turbidites thicker than 10 cm; Figure 7).

Through unit 2, turbidite frequency shows variations with three main phases of turbidite activity (Figure 7):

(a) From 9.2 to 5.5 ka cal. BP, turbidite activity is relatively continuous with almost 1 turbidite each 100 years (phase 1; Figure 7).
(b) From 5.5 to 3.8 ka cal. BP, the hypothesis of a sedimentary gap can be made (Figure 4), but there is no evidence of erosional surface attesting a major turbidite event. Then, we assumed that turbidite activity stopped abruptly, and no turbidites were deposited during this period (phase 2; Figure 7).
(c) From 3.8 ka cal. BP to modern, there was an increase in the turbidite activity with 31 turbidites recorded during this period, corresponding to 1 or 2 turbidites each 100 years (phase 3; Figure 7).

Sub-bottom seismic line

A sub-bottom seismic line was recovered during the MONOPOL cruise of the R/V Marion Dufresne through the eastern levee and the Active Channel (Figure 3b). The eastern levee is developed 83 m high and has a lateral extension of 30 km eastward. The top of the eastern levee is 45 m above the channel floor, and the bottom of the thalweg is characterized by chaotic facies (Figure 3, sequence A). The levee is constructed by successive overflows of gravity currents of the Active channel. Chaotic facies with strong acoustic signatures is visible in sequence A, which is the typical signature of HARP ("High Amplitude Reflection Packages") deposit (Flood et al., 1991; Pirmez and Flood, 1995). Sequence A attests to the first phase of construction of the Active Channel-levee complex. They were deposited after the breaching of the levee by unchannelized turbidity currents (Figure 3, sequence A).

The sub-bottom seismic lines show two major units in the levee of the Active Channel: the lower is characterized by continuous bedded facies with a medium acoustic signature (sequence B), and it is covered by a continuous bedded facies with a stronger acoustic signature (Figure 3, sequence C). Sequence B is crossed by gas presence or fluid escapements (Figure 3).

Core MD12-3417 being located on the seismic line makes it possible to link sedimentological units to acoustic units; unit 1 matches with the top of sequence B and sedimentary unit 2 with sequence C (Figure 3).

Discussion

First phase of construction of the Active Channel

The eastern levee is mainly constructed between 14.5 ka cal. BP (calibrated date from Weber et al., 1997) and 9.2 ka cal. BP (this study): the extremely high sedimentation rate during this period constructed a massive channel-levee complex (Figure 4), presumably in link with the rapid sea-level rise associated with the Meltwater pulse 1A (MWP-1A) in the North Atlantic (Weber et al., 1997). Only the period between 9.8 and 9.2 ka cal. BP was recovered by the core MD12-3417 and enabled to study the intense turbidite activity during this short time interval.

The global sea level from 14.5 ka to 9.2 ka cal. BP is between −95 and −20 m (Lambeck et al., 2014). The position of the −20-m isobath (Figure 1) is consistent with the idea of a good connection between the SoNG and the Ganges-Brahmaputra outlets until 9.2 ka cal. BP (Figure 1, sea-level location). Indo-Asian monsoon reconstructions during this period attest a relatively humid climate between 11 and 6 ka cal. BP according to the insolation variation and monsoonal proxies (Berkelhammer et al., 2012; Cai et al., 2012; Contreras-Rosales et al., 2014; Dykoski et al., 2005; Sarkar et al., 2015; Zorzi et al., 2015; Figures 2 and 7).

During the 600-year interval from 9.8 to 9.2 ka cal. BP, turbidite activity was intense, with 13–44 turbidites per 100 years, which corresponds to an average of 3 turbidites per 10 years (Figure 7). These turbidites are terrigenous, mainly composed by quartz, mica, and detrital calcite. These massive sediment supplies could only be explained by a quasi-continuous feeding of the deep system by rivers during this period. However, the dominance of reworked and broken pollen grains attests to a strong reworking of sediment previously deposited on the subaqueous delta or within the SoNG canyon, as opposed to direct fluvial input. Such results suggests that Ganges-Brahmaputra sediments were temporarily stored in the floodplain, the coastal delta plain, or the subaqueous delta (Rogers, 2012) and were reworked toward the SoNG or reworked from within the SoNG, which has been a major depocenter throughout the post-glacial and ultimately toward the Bengal fan, during periods of intense Indo-Asian monsoon precipitations and major river activity.

The combination between a good fluvial connection with the SoNG and heavy monsoon precipitations induced an intense turbidite activity and the development of levees of the Active Channel.

Although tectonic activity is recorded during the Holocene in the Ganges-Brahmaputra fluvial system and delta (Dortch et al., 2011; Kumar et al., 2006; Mugnier et al., 2011, 2011; Singh et al., 1997; Srivastava et al., 2009; Wang et al., 2014), no seismic events can be directly associated with a turbidite deposit in the Bengal fan: channelization of flows does not enable us to discriminate the tectonic origin of the gravity flow.

Abrupt sedimentary shift during the construction of the Active Channel

Our proxies indicate that the turbidite activity abruptly decreased at 9.2 ka cal. BP: what can explain this abrupt change in sedimentation (Figure 5)? A variation is notable in grain size distribution, which

impact variations in geochemical components, and we also distinguished a shift in the sediment color and magnetic susceptibility.

First, we could try to explain this shift by autocyclic forcings associated with the massive storage of sediment on the levees during the period of strong activity. Such intense activity caused the rapid vertical rise of the levees, which may have reached a threshold limit above which subsequent overflows of coarse material would have made it more difficult to overflow and deposit. If correct, this scenario would result in the gradual upward decrease in the grain size of the material that deposited on top of the levees. However, such a fining upward of material cannot be observed (Figure 5), and it was neither observed in previous studies (Morris et al., 2014; Skene et al., 2002). Alternatively, an upstream avulsion of the Active Channel could explain the abrupt change in sedimentary record, but there is no evidence of a more recent Active Channel in the upper fan.

Weber et al. (1997) detailed the construction of internal levees in the Active Channel older than 6 ka BP. Initiation of these internal levees attests to a decrease in flows or energy in the Active Channel and probably a decrease in the grain size of deposits. It is possible, therefore, that the initiation of internal levees in the Active Channel was correlated with the abrupt change in sedimentation that is observed in our record at 9.2 ka from the outer levee.

Around 9.2 ka cal. BP, there is no clear evidence of an abrupt climatic change in Indo-Asian monsoon proxies studied (Berkelhammer et al., 2012; Contreras-Rosales et al., 2014; Dykoski et al., 2005; Sarkar et al., 2015; Zorzi et al., 2015) that could suggest a direct impact of climate on turbidite activity and sediment delivery (Figure 2). Yet, this period is characterized by a rapid sea-level rise, described in Bangladesh and India (Banerjee, 1993; Hait and Behling, 2008; Islam and Tooley, 1999; Umitsu, 1993). Hait and Behling (2008) described a flooding of mangrove around 9.2 ka cal. BP in the coastal delta plain. However, it is difficult to separate the regional eustatic components contributing to these relative sea-level movements (Islam and Tooley, 1999).

With an abrupt sea-level rise at 9.2 ka, the accommodation space on the inner continental shelf would have became sufficient to develop the construction of the subaqueous delta and sediment would have been preferentially stored on the continental shelf, explaining the subsequent drastic reduction in the turbidite activity. Moreover, the subaerial delta is described as aggrading until 7 ka cal. BP which corresponds to the global sea-level stabilization (Goodbred and Kuehl, 1999), after which the delta progrades and initiates development of the subaqueous delta clinoform (Kuehl et al., 1997). Between the initiation of the Active Channel (14.5 ka cal. BP) and the abrupt shift (9.2 ka cal. BP), the delta constructed on the continental shelf could have been retrograding because of the transgressive phase (Grant et al., 2012), whereas after 9.2 ka cal. BP, the subaqueous delta could have become prograding because of the high sea-level position; such a change in sea level causes, therefore, a partial disconnection between the head of the SoNG and river mouth.

In our scenario, during the early-Holocene humid period, sea-level variations could explain the abrupt shift in sedimentation, with a transition between a first period of rapid fan accretion (before 9.2 ka cal. BP) with river discharges sufficient to keep pace with rapid sea level and a second period (after 9.2 ka cal. BP) with a sea level too high to be offset by Ganges-Brahmaputra discharges and a subaqueous delta building at the same time, storing sediment outlets and decreasing the sediment export to the Bengal fan.

Second period of turbidite activity

During the last 9.2 ka cal. BP, turbidite activity in the Active Channel was drastically reduced but still observed: the Ganges-Brahmaputra turbidite system has continuous activity. Our composite sedimentary record indicates an average frequency of 0–2 turbidites per 100 years during this period. These turbidites have a finer grain size distribution, but they are still terrigenous: quartz, mica, and detrital calcite prevailed and they attest of the major Ganges-Brahmaputra contribution.

Recent studies revealed that Ganges-Brahmaputra fluvial systems have evolved with the delta during the Holocene (Goodbred et al., 2014; Pickering et al., 2014). Between 11 and 7 ka cal. BP, the river mouths were directly feeding SoNG (Goodbred et al., 2014). Between 7 and 4 ka cal. BP, the Brahmaputra fluvial system is deflected toward the Sylhet basin where sediments can be stored because of the subsidence (Goodbred et al., 2014; Pickering et al., 2014). Finally, after 4 ka cal. BP, the Brahmaputra fluvial system returns to the Jamuna channel but discharges east of the SoNG, and the Ganges fluvial system shifted eastward (Goodbred et al., 2014; Pickering et al., 2014).

We propose that three phases took place during the last 9.2 ka cal. BP (Figure 7):

Phase 1 (9.2–5.5 ka cal. BP; Figure 7). The turbidite activity was continuous with around three turbidites per 500 years. Phase 1 is coeval with Holocene humid period with intensified SW monsoon and a succession of warmer and wetter conditions (Sarkar et al., 2015; Zorzi et al., 2015; Figure 7). Ganges-Brahmaputra delta was aggrading and became prograding with the stabilization of the global sea level around 7 ka BP (Goodbred and Kuehl, 1999). Even if turbidite activity was considerably reduced compared with the first phase, turbidites were still feeding the Active Channel. The enhanced Indo-Asian monsoon and the position of the Ganges and the Brahmaputra rivers during this period make the continuous feeding of the Active Channel possible. However, the regional sea-level rise and the construction of the subaqueous delta considerably reduced supplies into the Bengal fan. The idea that earthquakes and storms can induce a trigger of gravity flows into the deep system is not excluded, but there is no way to clearly identify the mechanism responsible for the turbidite deposits.

Phase 2 (5.5–4 ka cal. BP; Figure 7). The turbidite activity stopped during this period. This phase 2 appears to be roughly coeval with a period of weakening of the monsoon (Sarkar et al., 2015; Figure 8). The sea-level highstand was established during this period, and the subaqueous delta was prograding. Sea-level stabilization and weakening of the monsoon decreased sediment transfers, and sediments were more efficiently stored in the delta, which resulted in the decreased transfers toward the deep turbidite system. Moreover, between 7 and 4 ka cal. BP, the Brahmaputra river was routing toward the Sylhet basin, potentially decreasing sedimentary budget in the deep system (Figure 1; Goodbred et al., 2014).

Phase 3 (4 ka cal. BP to modern; Figure 7). Phase 3 is characterized by a recent increase in the turbidite activity (around five turbidites per 500 years). It is coeval with a relatively less humid period with oscillations between stronger and weaker Indo-Asian monsoon events (Gupta et al., 2003; Figure 7). During the last 4 ka cal. BP, the position of the Ganges-Brahmaputra fluvial systems would provide more important sediment supplies from rivers to deep turbidite system because of the vicinity with the head of the SoNG (Figure 1). The Brahmaputra river migration could explain the increase in turbidite activity during this period. Moreover, a study about adaptation and human migration underlines a shift of population toward the Ganges alluvial plain, around 4 ka cal. BP during the aridification period in India, coinciding with the appearance of rainy season crops (Gupta, 2004; Gupta et al., 2006). Gupta et al. (2006) suggested that during the last 2.5 ka cal. BP, intense agriculture and population pressure in the Ganges alluvial plain has led to a

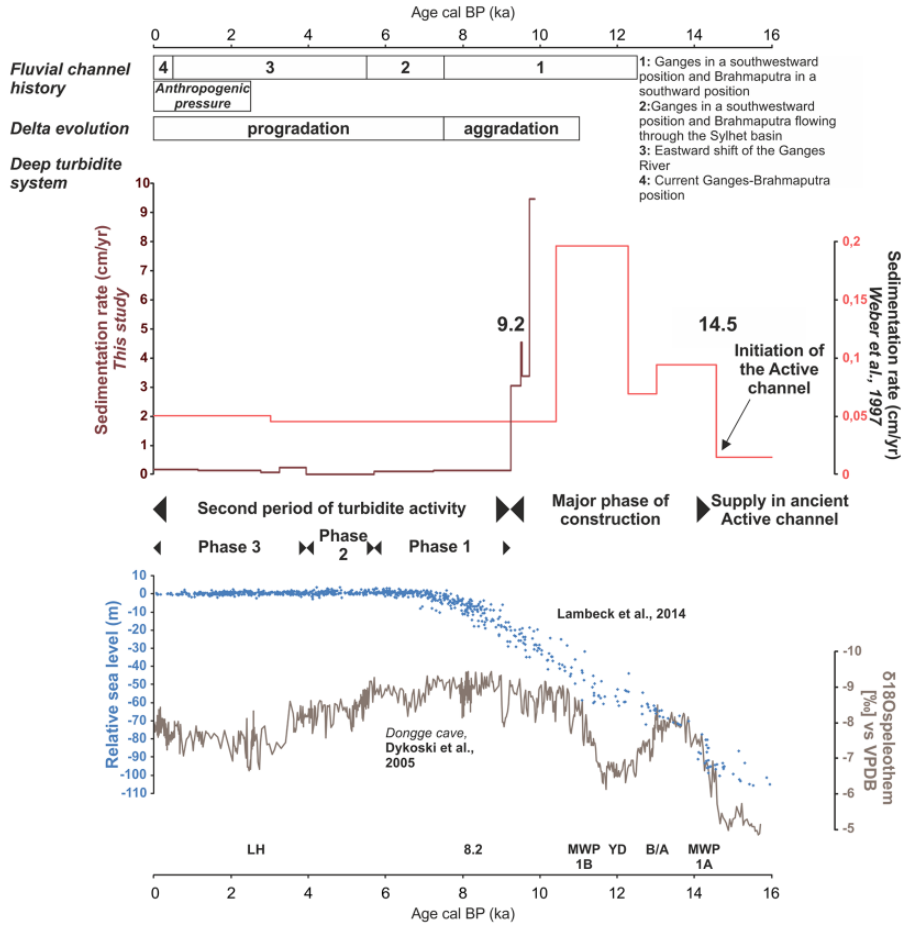

Figure 8. Initiation and evolution of the Active channel during the last 18 ka cal. BP. Comparison between the Ganges-Brahmaputra river's history, the delta evolution, the deep turbidite system represented by the sedimentation rate obtained by Weber et al. (1997) and in this study, phase of activity of the Active Channel, relative sea level (Lambeck et al., 2014), and Indo-Asian monsoon (Dykoski et al., 2005). Sedimentation rate curve of Weber et al. (1997) has been calibra+ted.

massive deforestation in this area. This almost complete extinction of forests would generate an increase in erosion processes and would increase Ganges discharges. This idea of a potential impact of human activity on the Active Channel sedimentation is supported by pollen analyses, which revealed that Borassus trees dominate around 1.1 ka cal. BP, attesting sediments from the alluvial and the coastal plain but maybe also crops expansion related to human activity.

Global history of the Active Channel

Initiation. Weber et al. (1997) have dated the initiation of the construction of the Active Channel around 14.5 ka cal. BP (12.800 years ^{14}C BP; Figure 8). The Active Channel is preceded by unchannelized flows depositing HARPs (Figure 3, sequence A). The avulsion process is responsible for the initiation of the Active Channel. Avulsion processes are controlled by several autocyclic forcings, such as asymmetry between levees, Coriolis effect, flow stripping, and preexisting bathymetry, and/or allocyclic forcings, such as eustasy or climatic variations. According to Curray et al. (2003), channel avulsions in the Ganges-Brahmaputra turbidite system mainly occurred in the area of highest sedimentation rates, which is consistent with an avulsion in the upper or middle fan. The Active Channel initiated around 14.5 ka cal. BP, synchronously with the increase in the Indo-Asian monsoon (Dykoski et al., 2005) and the rapid transgression phase associated with the MWP-1A (Weber et al., 1997; Figure 8). Massive river discharges at this period may have facilitated the breakup of an old levee and the avulsion of an ancient Active Channel.

Major phase of construction. During the first phase of construction, the Active Channel grew very rapidly. The combination between marine transgression and humid climate induced an intense turbidite activity and the main phase of development of levees of the Active Channel (Figures 3 and 8). According to Weber et al. (1997), turbidite sedimentation in the Active Channel was clearly linked to the global sea-level rise, but it seems that the Indo-Asian monsoon also affected the early construction of the Active Channel (Figure 8). Ganges-Brahmaputra discharges were directly transferred through the SoNG into the Bengal fan during this period.

At 9.2 ka cal. BP, a local increase in sea level partially disconnected the head of the canyon and river mouths, and despite of the massive river discharges that were likely associated with the humid climate, construction of the Active Channel reduced abruptly. The subaqueous delta begun its construction and stored a large part of sediments discharged by rivers (Figure 8). Weber et al. (1997) have dated the end of the major phase of construction at 10.4 ka cal. BP. Their dating framework did not make it possible to get a more precise estimate than ~10.4 ka cal. BP for the shift. Our study makes it possible to determine the age of the abrupt change in sedimentation more precisely at 9.2 ka cal. BP.

The Bengal fan dynamics seem similar to that of the Indus deep sea fan (Bourget et al., 2013; Prins et al., 2000; Prins and Postma, 2000). Turbidite sedimentation appears to be controlled by sea-level variations and monsoon variations, with sea-level rise causing a major decrease in sedimentation rates and turbidite frequency in both systems (Prins and Postma, 2000). Massive discharge of these two river systems are buffered by a wide

shelf, storing sediments and explaining that abrupt changes in sedimentation may be associated with sea-level variations in both the Bengal and the Indus fans (Clift et al., 2014; Prins and Postma, 2000).

Second period of turbidite activity. During the last 9.2 ka cal. BP, the sea-level was relatively stable (Grant et al., 2012): sedimentation rate declined drastically, but turbidite activity was still present with three distinct phases of activity. These three phases co-evolved with many forcings as well as Indo-Asian monsoon variations (Figures 7 and 8), Ganges-Brahmaputra rivers migrations, the delta construction, and the anthropogenic activity.

Conclusion

Through the recognition of turbidite deposits, the reconstruction of sedimentation rate, turbidite frequency, and turbidite thickness, the detailed sedimentological record obtained on the levee of the Active Channel during MONOPOL cruise of the R/V Marion Dufresne provides a new insight about the establishment of the Active Channel in the Bengal fan in the light of different autocyclic and allocyclic forcings during the Holocene. The following conclusions are reached:

1. The Active Channel has been initiated around 14.5 ka cal. BP (Weber et al., 1997). The position of the sea level and the strengthening of the Indo-Asian monsoon until 9.2 ka cal. BP enabled a strong connection between rivers and the Bengal fan and explained the high sedimentation rates and the rapid construction of well-developed levees.
2. At 9.2 ka cal. BP, the sea level reached a position from which massive sediment discharges were not large enough to compensate for the rise of sea level. The sedimentation rate declined abruptly in the Active Channel, and sediments were mainly stored in the subaqueous delta.
3. During the last 9.2 ka cal. BP, turbidite activity is still recorded but irregular. Weakening of the Indo-Asian monsoon, stabilization of the sea level, and intrinsic forcings as initiation of the delta and rivers routing impacted the turbidite activity. The anthropogenic impact can also be a hypothesis of forcing on the turbidite activity during the last 2.5 ka cal. BP.
4. Finally, it is really important not to oversimplify the construction of the Bengal fan with the Indo-Asian monsoon as unique and major forcing. The complexity and the combination of different forcings affecting transfers between Ganges-Brahmaputra fluvial system and the Bengal fan explained the activity of the deep turbidite system, especially the sea-level fluctuations.

Acknowledgements

We thank the MONOPOL ANR project (no. ANR 2011 Blanc SIMI 5-6 024 04) for the data, TOTAL, and Action Marges, the French margins project for the map contribution. We thank the 'ARTEMIS' technical platform for radiocarbon age dating. Finally, we are also grateful to EPOC technicians and engineers: P Lebleu, I Billy, O Ther, B Martin, B Cosson, L Rossignol, and MH Castera for the data acquisition. We acknowledge Lucia Hudson-Turner who provides English language support. Finally, two anonymous reviewers are thanked for their comments on the initial version of this manuscript.

Funding

The author(s) received no financial support for the research, authorship, and/or publication of this article.

References

Alam M (1989) Geology and depositional history of Cenozoic sediments of the Bengal Basin of Bangladesh. *Palaeogeography, Palaeoclimatology, Palaeoecology* 69: 125–139.

Allison MA, Khan SR, Goodbred SL Jr et al. (2003) Stratigraphic evolution of the late-Holocene Ganges–Brahmaputra lower delta plain. *Sedimentary Geology* 155: 317–342. DOI: 10.1016/S0037-0738(02)00185-9.

Anand A and Jain AK (1987) Earthquakes and deformational structures (seismites) in Holocene sediments from the Himalayan-Andaman Arc, India. *Tectonophysics* 133: 105–120. DOI: 10.1016/0040-1951(87)90284-8.

Banerjee PK (1993) Imprints of late quaternary climatic and sea level changes on East and South Indian coast. *Geo-Marine Letters* 13: 56–60. DOI: 10.1007/BF01204393.

Berkelhammer M, Sinha A, Stott L et al. (2012) An abrupt shift in the Indian monsoon 4000 years ago. *Climates, Landscapes, and Civilizations* 198: 75–88.

Blaauw M (2010) Methods and code for 'classical' age-modelling of radiocarbon sequences. *Quaternary Geochronology* 5: 512–518.

Bonneau L, Jorry SJ, Toucanne S et al. (2014) Millennial-Scale response of a Western Mediterranean river to late Quaternary climate changes: A view from the deep sea. *The Journal of Geology* 122: 687–703. DOI: 10.1086/677844.

Bouma AH, Kuenen PH and Shepard FP (1962) *Sedimentology of Some Flysch Deposits: A Graphic Approach to Facies Interpretation*. Amsterdam: Elsevier.

Bourget J, Zaragosi S, Ellouz-Zimmermann S et al. (2010) Highstand vs. lowstand turbidite system growth in the Makran active margin: Imprints of high-frequency external controls on sediment delivery mechanisms to deep water systems. *Marine Geology* 274: 187–208. DOI: 10.1016/j.margeo.2010.04.005.

Bourget J, Zaragosi S, Rodriguez M et al. (2013) Late Quaternary megaturbidites of the Indus Fan: Origin and stratigraphic significance. *Marine Geology* 336: 10–23. DOI: 10.1016/j.margeo.2012.11.011.

Cai Y, Zhang H, Cheng H et al. (2012) The Holocene Indian monsoon variability over the southern Tibetan Plateau and its teleconnections. *Earth and Planetary Science Letters* 335–336: 135–144. DOI: 10.1016/j.epsl.2012.04.035.

Clift PD, Giosan L, Henstock TJ et al. (2014) Sediment storage and reworking on the shelf and in the Canyon of the Indus River-Fan System since the last glacial maximum. *Basin Research* 26: 183–202. DOI: 10.1111/bre.12041.

Contreras-Rosales LA, Jennerjahn T, Tharammal T et al. (2014) Evolution of the Indian Summer Monsoon and terrestrial vegetation in the Bengal region during the past 18 ka. *Quaternary Science Reviews* 102: 133–148. DOI: 10.1016/j.quascirev.2014.08.010.

Croudace IW, Rindby A and Rothwell RG (2006) ITRAX: Description and evaluation of a new multi-function X-ray core scanner. *Geological Society, London, Special Publications* 267: 51–63.

Curray JR, Emmel FJ and Moore DG (2003) The Bengal Fan: Morphology, geometry, stratigraphy, history and processes. *Marine and Petroleum Geology* 19: 1191–1223. DOI: 10.1016/s0264-8172(03)00035-7.

Dortch JM, Dietsch C, Owen LA et al. (2011) Episodic fluvial incision of rivers and rock uplift in the Himalaya and Transhimalaya. *Journal of the Geological Society* 168: 783–804. DOI: 10.1144/0016-76492009-158.

Dutta K, Bhushan R and Somayajulu BLK (2001) ΔR correction values for the northern Indian Ocean. *Radiocarbon* 43: 483–488.

Dykoski CA, Edwards RL, Cheng H et al. (2005) A high-resolution, absolute-dated Holocene and deglacial Asian monsoon record from Dongge Cave, China. *Earth and Planetary Science Letters* 233: 71–86. DOI: 10.1016/j.epsl.2005.01.036.

Dypvik H and Harris NB (2001) Geochemical facies analysis of fine-grained siliciclastics using Th/U, Zr/Rb and (Zr+Rb)/Sr ratios. *Chemical Geology* 181: 131–146. DOI: 10.1016/S0009-2541(01)00278-9.

Emmel FJ and Curray JR (1983) The Bengal Submarine Fan, Northeastern Indian ocean. *Geo-Marine Letters* 3: 119–124.

Flood RD, Manley PL, Kowsmann RO et al. (1991) Seismic facies and late Quaternary growth of Amazon submarine fan. In: Weimer P and Link MH (eds) *Seismic Facies and Sedimentary Processes of Submarine Fans and Turbidite Systems* (Frontiers in sedimentary geology). New York: Springer, pp. 415–433.

Goldfinger C, Morey AE, Nelson CH et al. (2007) Rupture lengths and temporal history of significant earthquakes on the offshore and north coast segments of the Northern San Andreas Fault based on turbidite stratigraphy. *Earth and Planetary Science Letters* 254: 9–27. DOI: 10.1016/j.epsl.2006.11.017.

Goodbred SL Jr and Kuehl SA (1999) Holocene and modern sediment budgets for the Ganges-Brahmaputra river system: Evidence for highstand dispersal to flood-plain, shelf, and deep-sea depocenters. *Geology* 27: 559–562. DOI: 10.1130/0091-7613(1999)027<0559:HAMSBF>2.3.CO;2.

Goodbred SL Jr and Kuehl SA (2000a) Enormous Ganges-Brahmaputra sediment discharge during strengthened early Holocene monsoon. *Geology* 28: 1083–1086. DOI: 10.1130/0091-7613(2000)28<1083:egsdds>2.0.co;2.

Goodbred SL Jr and Kuehl SA (2000b) The significance of large sediment supply, active tectonism, and eustasy on margin sequence development: Late Quaternary stratigraphy and evolution of the Ganges–Brahmaputra delta. *Sedimentary Geology* 133: 227–248. DOI: 10.1016/S0037-0738(00)00041-5.

Goodbred SL Jr, Kuehl SA, Steckler MS et al. (2003) Controls on facies distribution and stratigraphic preservation in the Ganges–Brahmaputra delta sequence. *Sedimentary Geology* 155: 301–316.

Goodbred SL Jr, Paolo PM, Ullah MS et al. (2014) Piecing together the Ganges-Brahmaputra-Meghna River delta: Use of sediment provenance to reconstruct the history and interaction of multiple fluvial systems during Holocene delta evolution. *The Geological Society of America Bulletin* 126: 1495–1510.

Grant K, Rohling E, Bar-Matthews M et al. (2012) Rapid coupling between ice volume and polar temperature over the past 150,000 [thinsp] years. *Nature* 491: 744–747.

Gupta AK (2004) Origin of agriculture and domestication of plants and animals linked to early Holocene climate amelioration. *Current Science* 87: 54–59.

Gupta AK, Anderson DM and Overpeck JT (2003) Abrupt changes in the Asian southwest monsoon during the Holocene and their links to the North Atlantic Ocean. *Nature* 421: 354–357. DOI: 10.1038/nature01340.

Gupta AK, Anderson DM, Pandey DN et al. (2006) Adaptation and human migration, and evidence of agriculture coincident with changes in the Indian summer monsoon during the Holocene. *Current Science* 90: 1082–1090.

Hait AK and Behling H (2008) Holocene mangrove and coastal environmental changes in the western Ganga–Brahmaputra Delta, India. *Vegetation History and Archaeobotany* 18: 159–169. DOI: 10.1007/s00334-008-0203-5.

Hubscher C, Spiess V, Breitzke M et al. (1997) The youngest channel-levee system of the Bengal Fan: Results from digital sediment echosounder data. *Marine Geology* 141: 125–145. DOI: 10.1016/s0025-3227(97)00066-2.

Islam MS and Tooley MJ (1999) Coastal and sea-level changes during the Holocene in Bangladesh. *Quaternary International* 55: 61–75. DOI: 10.1016/S1040-6182(98)00025-1.

Kolla V, Bandyopadhyay A, Gupta P et al. (2012) Morphology and internal structure of a recent upper Bengal Fan-Valley complex. In: Prather BE, Deptuck ME, Mohrig D et al. (eds) *Application of the Principles of Seismic Geomorphology to Continental-Slope and Base-of-Slope Systems: Case Studies from Seafloor and near-Seafloor Analogues*. Tulsa, OK: SEPM Society for Sedimentary Geology (SEPM Special Publication 99), pp. 347–369.

Kottke B, Schwenk T, Breitzke M et al. (2003) Acoustic facies and depositional processes in the upper submarine canyon Swatch of No Ground (Bay of Bengal). *Deep Sea Research Part II: Topical Studies in Oceanography* 50: 979–1001. DOI: 10.1016/s0967-0645(02)00616-1.

Kudrass HR, Hofmann A, Doose H et al. (2001) Modulation and amplification of climatic changes in the Northern Hemisphere by the Indian summer monsoon during the past 80 k.y. *Geology* 29: 63–66. DOI: 10.1130/0091-7613(2001)029<0063:MAAOCC>2.0.CO;2.

Kudrass HR, Michels KH, Wiedicke M et al. (1998) Cyclones and tides as feeders of a submarine canyon off Bangladesh. *Geology* 26: 715–718. DOI: 10.1130/0091-7613(1998)026<0715:CATAFO>2.3.CO;2.

Kuehl SA, Hariu TM and Moore WS (1989) Shelf sedimentation off the Ganges-Brahmaputra river system: Evidence for sediment bypassing to the Bengal fan. *Geology* 17: 1132–1135.

Kuehl SA, Levy BM, Moore WS et al. (1997) Subaqueous delta of the Ganges-Brahmaputra river system. *Marine Geology* 144: 81–96. DOI: 10.1016/S0025-3227(97)00075-3.

Kumar S, Wesnousky SG, Rockwell TK et al. (2006) Paleoseismic evidence of great surface rupture earthquakes along the Indian Himalaya. *Journal of Geophysical Research: Solid Earth* 111: B03304, DOI: 10.1029/2004JB003309.

Lambeck K, Rouby H, Purcell A et al. (2014) Sea level and global ice volumes from the Last Glacial Maximum to the Holocene. *Proceedings of the National Academy of Sciences* 111: 15296–15303. DOI: 10.1073/pnas.1411762111.

Lambeck K, Woodroffe CD, Antonioli F et al. (2010) Paleoenvironmental records, geophysical modelling and reconstruction of sea level trends and variability on centennial and longer timescales. In: Church JA, Woodworth PL, Aarup T et al. (eds) *Understanding Sea-Level Rise and Variability*. Oxford: Wiley-Blackwell, pp. 61–121.

Lowe DR (1975) Water escape structures in coarse-grained sediments. *Sedimentology* 22: 157–204. DOI: 10.1111/j.1365-3091.1975.tb00290.x.

Milliman JD and Syvitski JPM (1992) Geomorphic/Tectonic control of sediment discharge to the ocean: The importance of small mountainous rivers. *The Journal of Geology* 100: 525–544.

Morgan JP and McIntire WG (1959) Quaternary geology of the Bengal basin, East Pakistan and India. *Geological Society of America Bulletin* 70: 319–342.

Morris EA, Hodgson DM, Brunt RL et al. (2014) Origin, evolution and anatomy of silt-prone submarine external levées. *Sedimentology* 61: 1734–1763. DOI: 10.1111/sed.12114.

Mugnier JL, Huyghe P, Gajurel AP et al. (2011) Seismites in the Kathmandu basin and seismic hazard in central Himalaya. *Tectonophysics* 509: 33–49. DOI: 10.1016/j.tecto.2011.05.012.

Palamenghi L, Schwenk T, Spiess V et al. (2011) Seismostratigraphic analysis with centennial to decadal time resolution of the sediment sink in the Ganges-Brahmaputra subaqueous delta. *Continental Shelf Research* 31: 712–730. DOI: 10.1016/j.csr.2011.01.008.

Pate RD, Goodbred SL Jr and Khan SR (2009) Delta double-stack: Juxtaposed Holocene and Pleistocene sequences from the Bengal Basin, Bangladesh. *The Sedimentary Record* 7: 4–9.

Pickering JL, Goodbred SL Jr, Reitz MD et al. (2014) Late Quaternary sedimentary record and Holocene channel avulsions of the Jamuna and Old Brahmaputra River valleys in the upper Bengal delta plain. *Geomorphology* 227: 123–136.

Pirmez C and Flood RD (1995) Morphology and structure of Amazon Channel. *Proceedings of the Ocean Drilling Program: Initial Reports* 155: 23–45.

Poddar MC (1952) Preliminary report of the Assam earthquake, 15th August, 1950. *Bulletin of the Geological Society of India* 2: 11–13.

Prins MA and Postma G (2000) Effects of climate, sea level, and tectonics unraveled for last deglaciation turbidite records of the Arabian Sea. *Geology* 28: 375–378. DOI: 10.1130/0091-7613(2000)28<375:EOCSLA>2.0.CO;2.

Prins MA, Postma G, Cleveringa J et al. (2000) Controls on terrigenous sediment supply to the Arabian Sea during the late Quaternary: The Indus Fan. *Marine Geology* 169: 327–349. DOI: 10.1016/s0025-3227(00)00086-4.

Rashid T, Suzuki S, Sato H et al. (2013) Relative sea-level changes during the Holocene in Bangladesh. *Journal of Asian Earth Sciences* 64: 136–150. DOI: 10.1016/j.jseaes.2012.12.007.

Reimer PJ, Bard E, Bayliss A et al. (2013) IntCal13 and Marine13 radiocarbon age calibration curves 0-50,000 years cal BP. *Radiocarbon* 55(4): 1889–1903.

Reitz MD, Pickering JL, Goodbred SL Jr et al. (2015) Effects of tectonic deformation and sea level on river path selection: Theory and application to the Ganges-Brahmaputra-Meghna River Delta. *Journal of Geophysical Research: Earth Surface* 120: 671–689. DOI: 10.1002/2014JF003202.

Rogers KG (2012) Spatial and temporal sediment distribution from river mouth to remote depocenters in the Ganges-Brahmaputra delta, Bangladesh. PhD thesis. Nashville, TN: Vanderbilt University (unpublished).

Rogers KG, Goodbred SL Jr and Khan SR (2015) Shelf-to-canyon connections: Transport-related morphology and mass balance at the shallow-headed, rapidly aggrading Swatch of No Ground (Bay of Bengal). *Marine Geology* 369: 288–299.

Rogers KG, Goodbred SL Jr and Mondal DR (2013) Monsoon sedimentation on the 'abandoned' tide-influenced Ganges–Brahmaputra delta plain. *Estuarine, Coastal and Shelf Science* 131: 297–309. DOI: 10.1016/j.ecss.2013.07.014.

Sarkar S, Prasad S, Wilkes H et al. (2015) Monsoon source shifts during the drying mid-Holocene: Biomarker isotope based evidence from the core 'monsoon zone' (CMZ) of India. *Quaternary Science Reviews* 123: 144–157. DOI: 10.1016/j.quascirev.2015.06.020.

Singh I, Rajagopalan G, Agarwal K et al. (1997) Evidence of Middle to Late-Holocene neotectonic activity in the Ganga Plain. *Current Science* 73: 1114–1117.

Skene KI, Piper DJW and Hill PS (2002) Quantitative analysis of variations in depositional sequence thickness from submarine channel levees. *Sedimentology* 49: 1411–1430. DOI: 10.1046/j.1365-3091.2002.00506.x.

Skinner LC and McCave IN (2003) Analysis and modelling of gravity- and piston coring based on soil mechanics. *Marine Geology* 199: 181–204. DOI: 10.1016/s0025-3227(03)00127-0.

Sømme TO, Helland-Hansen W, Martinsen OJ et al. (2009) Relationships between morphological and sedimentological parameters in source-to-sink systems: A basis for predicting semi-quantitative characteristics in subsurface systems. *Basin Research* 21: 361–387. DOI: 10.1111/j.1365-2117.2009.00397.x.

Southon J, Kashgarian M, Fontugne M et al. (2002) Marine reservoir corrections for the Indian Ocean and Southeast Asia. *Radiocarbon* 44: 167–180.

Srivastava P, Bhakuni SS, Luirei K et al. (2009) Morpho-sedimentary records at the Brahmaputra River exit, NE Himalaya: Climate–tectonic interplay during the Late Pleistocene–Holocene. *Journal of Quaternary Science* 24: 175–188. DOI: 10.1002/jqs.1190.

St-Onge G, Mulder T, Francus P et al. (2007) Chapter two continuous physical properties of cored marine sediments. *Developments in Marine Geology* 1: 63–98.

Thomas B, Despland P and Holmes L (2012) Submarine sediment distribution patterns within the Bengal fan system, deep water Bengal basin, India. AAPG International Convention and Exhibition, Singapore, 16–19 September 2012.

Toucanne S, Zaragosi S, Bourillet J-F et al. (2012) External controls on turbidite sedimentation on the glacially-influenced Armorican margin (Bay of Biscay, western European margin). *Marine Geology* 303–306: 137–153. DOI: 10.1016/j.margeo.2012.02.008.

Umitsu M (1993) Late quaternary sedimentary environments and landforms in the Ganges Delta. *Sedimentary Geology* 83: 177–186. DOI: 10.1016/0037-0738(93)90011-S.

Wang P, Chen J, Dai F et al. (2014) Chronology of relict lake deposits around the Suwalong paleolandslide in the upper Jinsha River, SE Tibetan Plateau: Implications to Holocene tectonic perturbations. *Geomorphology* 217: 193–203. DOI: 10.1016/j.geomorph.2014.04.027.

Weber ME, Wiedicke MH, Kudrass HR et al. (1997) Active growth of the Bengal Fan during sea-level rise and highstand. *Geology* 25: 315–318. DOI: 10.1130/0091-7613(1997)025<0315:agotbf>2.3.co;2.

Wedepohl KH and Correns CW (1969) *Handbook of Geochemistry*. New York: Springer.

Zaragosi S, Bourillet J-F, Eynaud F et al. (2006) The impact of the last European deglaciation on the deep-sea turbidite systems of the Celtic-Armorican margin (Bay of Biscay). *Geo-Marine Letters* 26: 317–329. DOI: 10.1007/s00367-006-0048-9.

Zorzi C, Sanchez Goñi MF, Anupama K et al. (2015) Indian monsoon variations during three contrasting climatic periods: The Holocene, Heinrich Stadial 2 and the last interglacial–glacial transition. *Quaternary Science Reviews* 125: 50–60. DOI: 10.1016/j.quascirev.2015.06.009.